Using Nanowires To Extract Excitons from a Nanocrystal Solid

August Dorn,* David B. Strasfeld, Daniel K. Harris, Hee-Sun Han, and Moungi G. Bawendi

Department of Chemistry, Massachusetts Institute of Technology, Cambridge, Massachusetts 02139, United States

ABSTRACT

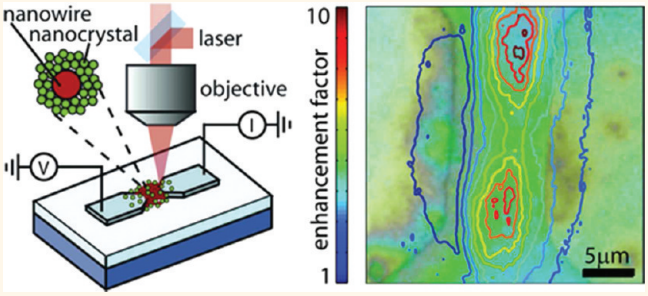

Synthetic methods yielding highly uniform colloidal semiconductor nanocrystals with controlled shapes and sizes are now available for many materials. These methods have enabled geometrical control of optical properties, which are difficult or impossible to achieve in conventional bulk solids. However, incorporating nanocrystals efficiently into photodetectors remains challenging because of the low charge carrier mobilities typical of nanocrystal solids. Here we present an approach based on exciton energy transfer from CdSe/CdS core/shell nanocrystals to embedded CdSe nanowires. By combining the wide electronic tunability of nanocrystals with the excellent one-dimensional charge transport characteristics obtainable in nanowires, we are able to increase photocurrent extraction from a nanocrystal solid by 2—3 orders of magnitude. Furthermore, we correlate local device morphology with optoelectronic functionality by measuring the local photocurrent response in a scanning confocal microscope. We also discuss how nancocrystal/nanowire hybrid devices could be used in particle detector systems.

KEYWORDS: nanowire · nanocrystal · energy transfer · FRET · cadmium selenide · CdSe

Nanocrystals have attracted considerable interest as the active media in photodetector systems, owing to their tunable effective band gaps.[1−5] However, solids and thin films composed of nanocrystals typically exhibit low mobilities as a consequence of inter-nanocrystal hopping transport, the dominant charge carrier conduction mechanism in these material systems.[1,2,6] Photodetectors with nanocrystals as the active media could therefore benefit from new schemes for efficiently extracting photocurrent from a nanocrystal solid.

In this study, we explore how the photocurrent extraction challenge in nanocrystal solids can be overcome by using a CdSe/CdS nanocrystal—CdSe nanowire hybrid photodetector device as a model system. The excitons created by radiation interacting with the nanocrystal solid are nonradiatively transferred to the embedded nanowires contacted between electrodes, leading to a photocurrent signal. We thus take advantage of the wide electronic tunability of nanocrystals combined with the large surface areas and high charge carrier mobilities afforded by nanowires. Related systems have previously been studied in the context of solar cells,[7−9] for carbon-nanotube-based devices,[10,11] in molecular systems[12] and in devices with single quantum dots embedded in nanowires.[13] For a proof of principle, we used a scanning confocal microscope to locally illuminate the device (see Figure 1a). The resulting photocurrent was recorded as a function of focal point position. The bare CdSe nanowire photodetectors were fabricated by the electrically controlled solution—liquid—solid (EC-SLS) growth process,[14,15] which is an extension of the solution—liquid—solid (SLS) mechanism.[16−19] The EC-SLS method is well-suited for device fabrication because nanowires are grown directly between metal electrodes. This yields functioning devices, such as photodetectors, in a single fabrication step. Nanowire diameters in our devices were on the order of 20 nm, which is approximately twice the exciton Bohr diameter of 11.2 nm in CdSe. Therefore, the observed absorption edge of the nanowires around 713 nm is the same as for bulk CdSe.[20−22] Colloidal CdSe/CdS nanocrystals with an absorption edge around 550 nm were synthesized using standard wet-chemical techniques and were subsequently deposited by drop-casting. The resulting nanocrystal thin films had a thickness of approximately 50 nm (see also Supporting Information). The difference in absorption spectrum between the nanowires and nanocrystals ensured that at an

* Address correspondence to adorn@physnet.uni-hamburg.de.

Received for review August 22, 2011 and accepted October 17, 2011.

Published online October 17, 2011
10.1021/nn203227t

© 2011 American Chemical Society

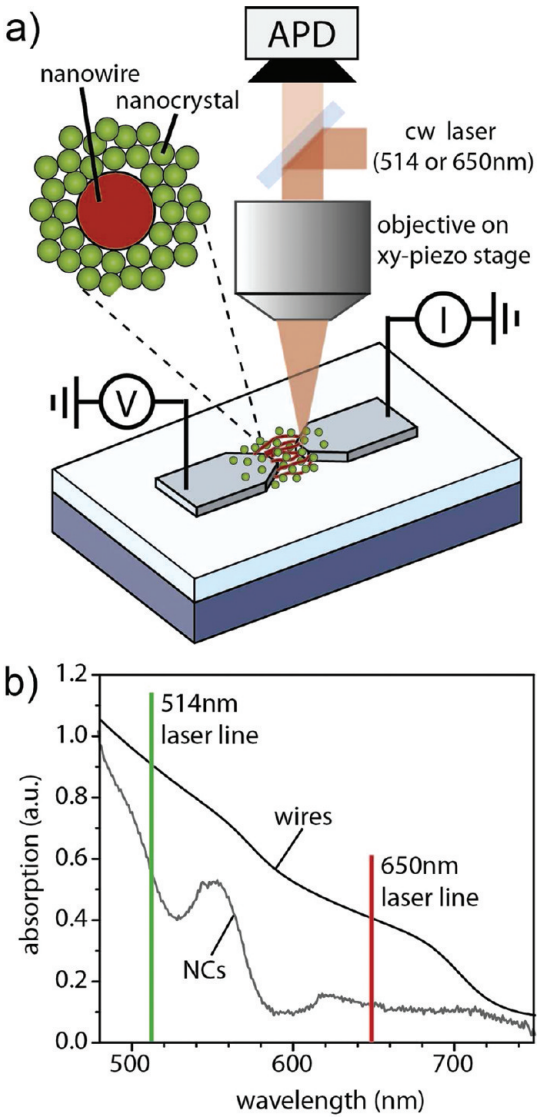

Figure 1. Experimental setup. (a) Schematic of a nanocrystal/nanowire hybrid device and the confocal photocurrent scanning measurement setup. (b) Optical absorption spectra of a bare CdSe nanowire mat and of a drop-cast CdSe/CdS nanocrystal film without nanowires.

excitation wavelength of 650 nm *only* the nanowires could absorb light, whereas at 514 nm excitons can be created in the nanocrystals *and* nanowires (see also Figure 1b).

RESULTS

A wide field optical microscope image of a device taken under white light illumination, as well as an image acquired by recording the reflected light in a confocal scan at 650 nm, is presented in Figure 2a,b. Since the nanocrystals form a homogeneous film covering the entire device, the darker regions in Figure 2a are indicative of higher nanowire coverage. Photocurrent maps taken at 514 and 650 nm of the same device area before nanocrystals were deposited are shown in Figure 2c,d, and the corresponding measurements after drop-casting nanocrystals are presented in Figure 2e,f. All measurements were taken under the same conditions at a constant bias of 1 V and under continuous wave laser illumination at 10 μW. A homogeneous nanowire mat could be expected to show a photocurrent maximum when the laser focus is placed at the center between the electrodes because charge carriers from excitons created in the center of the device have the largest number of pathways to connect to the electrodes. On the other hand, for inhomogeneous nanowire coverage, the regions with higher nanowire density will also have a higher absorption cross section leading to a higher photocurrent response. The overall photocurrent induced by illuminating a specific location is therefore a combination of the local light absorption efficiency coupled with the ease of photocurrent extraction from that point. Our model is consistent with the photocurrent maps in Figure 2c–f, where the photocurrent is largely centered between the two electrodes, with a shift toward the left electrode, which also has a higher nanowire density at its edge, owing to the fabrication process (compare with Figure 2a). Previous reports of scanning photocurrent measurements on nanowire-based devices have sometimes observed enhancements when the laser focus was positioned close to the electrode edges, resulting from Schottky barriers at the contacts.[23–26] This effect is not prominent in our devices, indicating ohmic contacts between the nanowires and the metal electrodes.

A striking feature in our measurements is the strong enhancement in photocurrent observed when scanning at 514 nm after drop-casting nanocrystals onto the nanowire mat (compare Figure 2c,e). This enhancement is not observed when scanning at 650 nm (compare Figure 2d,f) because the nanocrystals are transparent at this wavelength and photocurrent only results from direct light absorption by the nanowires. The slight decrease in photocurrent at 650 nm after drop-casting, as seen when comparing Figure 2d,f, could be due to changes in reflectivity and refraction caused by the nanocrystal film. Control experiments with devices containing only nanocrystals and no wires showed photocurrents below 0.1 pA, the resolution limit of our setup.

In order to gain a more quantitative understanding of the photocurrent enhancement observed at 514 nm, we plot the ratio of the photocurrent maps taken before and after drop-casting nanocrystals in Figure 3a. Contour lines of the enhancement factors shown in Figure 3a are superimposed on an optical wide field image of the device under white light illumination in Figure 3b. Interestingly, photocurrent enhancement factors are largest in device regions with the *lowest* wire density. In contrast, the overall photocurrent seen in Figure 2c,e is largest in device areas with the *highest* wire density. In the following, we will analyze the processes and parameters relevant to the photocurrent

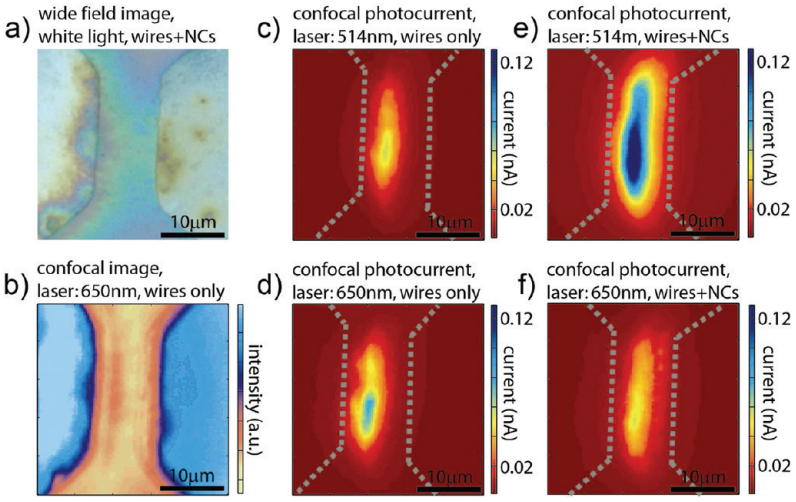

Figure 2. Scanning confocal photocurrent mapping. (a) Wide field optical microscope image of the device under white light illumination. (b) Scanning confocal image from reflected light at an excitation wavelength of 650 nm of the same device area as in (a). (c−f) Photocurrent maps of the same device area as in (a) and (b) at excitation wavelengths of 514 and 650 nm, as well as before and after drop-casting nanocrystals onto the nanowire mat. Every map consists of 100 × 100 data points spaced by 300 nm. All measurements were taken at 1 V bias and at a light intensity of 10 μW, scale bars = 10 μm.

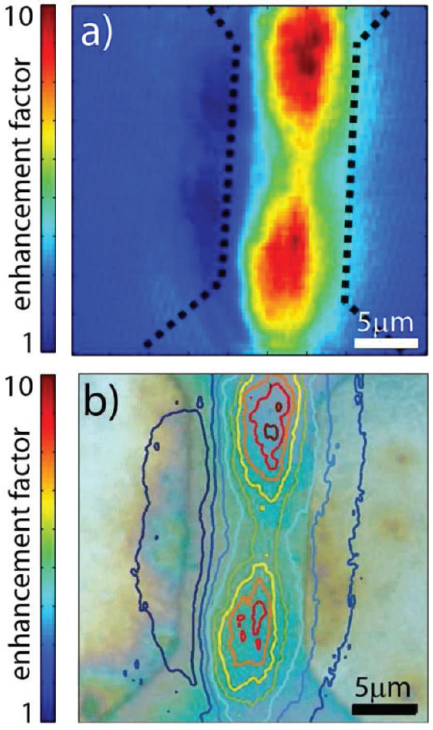

Figure 3. Local photocurrent enhancement factors. (a) Ratio of photocurrent maps before and after drop-casting nanocrystals taken at an excitation wavelength of 514 nm. The original data sets shown in Figure 2c,e were cropped and shifted for alignment. (b) Contour lines from the data set shown in (a) superimposed on an optical wide field image of the device under white light illumination.

enhancement described above. Clearly, photocurrent enhancement by depositing a nanocrystal film is only possible if the light absorption efficiency of the plain nanowire detector at the wavelength of interest is significantly smaller than unity. In other words, the maximum photocurrent enhancement achievable by adding nanocrystals is given by the reciprocal of the absorption efficiency of the plain nanowire detector. This is why regions with dense nanowire coverage at the edge of the left electrode (see Figure 3b) show very high photocurrents but almost no photocurrent enhancement after drop-casting nanocrystals. On the other hand, in the limit of very low wire coverage, the photocurrent is also low, but the enhancement factors after drop-casting nanocrystals are high and exceed 10 in some regions of the device. If the light absorption cross section of a nanowire is assumed to be proportional to its volume, a 50 nm thick nanocrystal film coating a nanowire of 20 nm diameter would lead to an enhancement factor of about 36. The actual enhancement factor, however, will be lower owing to incomplete exciton energy transfer to the nanowire, lower absorption by the nanocrystal film as compared to bulk CdSe, and varying light intensity along the device cross section resulting from absorption. The maximum observed enhancement factors of about 10 in our device could therefore be at or close to the single wire limit. In addition, the absolute value of the photocurrent in this region of the device is 2−3 orders of magnitude larger than the corresponding photocurrent of 0.1 pA (detection limited) in the plain nanocrystal device without wires. In other words, exciton extraction from the nanocrystal solid is enhanced by at least 2−3 orders of magnitude by the nanowires, while the contribution from direct absorption by the nanowires is below 10% in device regions with low nanowire density.

DISCUSSION

One of the largest obstacles to achieving complete exciton extraction from a nanocrystal solid using

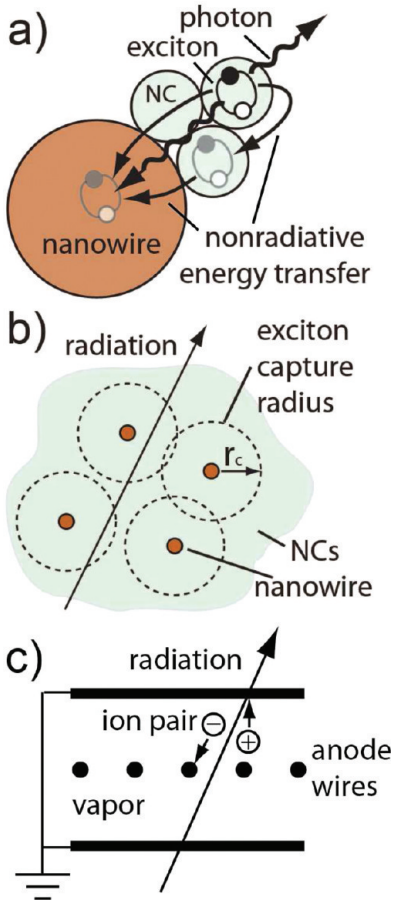

Figure 4. Exciton energy transfer and devices. (a) Schematic illustrating exciton energy transfer between nanocrystals and from nanocrystals to a nanowire, including possible radiative pathways. (b) Schematic of a cross section through a nanocrystal solid with embedded nanowires for photocurrent extraction. (c) Schematic of a wire chamber detector.

nanowires is incomplete exciton energy transfer from the nanocrystals to the nanowires. In order to contribute to photocurrent, the location of exciton creation within the nanocrystal solid has to be close enough to a wire to ensure efficient exciton capture through a combination of exciton diffusion within the nanocrystal solid and subsequent energy transfer to the nanowire (Figure 4a). In principle, charge separation at the nanocrystal/nanowire interface, radiative energy transfer, and nonradiative exciton transfer could play important roles in this process. However, charge separation at the nanocrystal/nanowire interface is improbable because the band alignment of the CdSe nanocrystals relative to the CdSe nanowires does not form a type II interface. In addition, this mechanism would lead to local charging within the nanocrystal film because of the extremely low conductivity of nanocrystal solids. As a result, local charging of the nanocrystal film would lead to higher exciton quenching within the nanocrystal film and a subsequent reduction in photocurrent. Radiative decay of excitons is not likely to play a significant role because the radiative lifetime of an isolated nanocrystal, which is about 25 ns, is 2−3 orders of magnitude longer than the exciton transfer lifetime between two adjacent nanocrystals, which we calculated to be about 180 ps (see Supporting Information). Therefore, nonradiative exciton energy transfer between nanocrystals and from nanocrystals to nanowires is probably the dominant mechanism in our device. While excitons are relatively free to diffuse within a monodisperse nanocrystal solid, energy transfer from a nanocrystal to a nanowire is irreversible because of lower exciton energies within the nanowires. This effectively leads to exciton funneling from the nanocrystal solid to the nanowires for excitons created within a capture radius R_c from a nanowire. The capture radius R_c is given by a convolution of the exciton diffusion length within the nanocrystal solid and the energy transfer radius from a nanocrystal to a nanowire. To ensure optimal detection efficiency of radiation quanta passing through the nanocrystal solid, it is therefore desirable to have nanowires separated by less than twice the exciton capture radius R_c (see Figure 4b). Obtaining a good quantitative value for the exciton capture radius requires more data on exciton diffusion lengths in nanocrystal solids, which could then be incorporated into analytical models.[27]

When comparing Figure 4b,c, it is evident that our device is conceptually similar to a Geiger counter or wire chamber in which the metal wires have been replaced by semiconductor nanowires, and the detection medium is a nanocrystal solid instead of a vapor. Indeed, the scheme described above could also be used to detect radiation other than optical photons because many types of particles create excitons when they interact with matter. This is of interest because nanocrystals offer unique material properties not available in conventional bulk solids. In particular, the size-tunable optical and electronic properties of nanocrystals offer new combinations of atomic number, band gap, electron and hole effective masses, g-factors, and magnetic properties that could be of interest for optimizing radiation/matter interactions.[28,29] A particularly promising approach appears to be using quantum confinement to increase the band gaps of semiconductors containing elements with high atomic numbers (*e.g.*, PbTl, bulk band gap ~0.3 eV) in order to combine high X-ray detection cross sections with exciton energies that allow for good detectability at room temperature. Nanocrystal/nanowire hybrid devices are therefore also a promising route to using nanocrystals as active media in particle detector systems.

In conclusion, nanocrystal/nanowire hybrid devices combine the broad electronic tunability of colloidal semiconductor nanocrystals with the large surface area and high charge carrier mobilities of nanowires. As a proof of concept, we studied photocurrent maps of a CdSe nanowire mesh sensitized with a layer of CdSe/CdS

nanocrystals using a confocal scanning microscope. Performing photocurrent scans at wavelengths above and below the nanocrystal absorption band edge, we were able to demonstrate up to 10-fold enhancement from nonradiative energy transfer from the nanocrystals to the nanowires. This corresponds to a contribution from direct nanowire light absorption to the overall photocurrent of 10% for low nanowire density. Importantly, the nanowires enhance photocurrent extraction from than nanocrystal solid by 2−3 orders of magnitude as compared to plain nanocrystal devices without nanowires. In the devices presented here, both the nanocrystals and nanowires consisted of CdSe, serving as an example of how shape, size, and dimensionality can be used to tailor the properties and functionality of a material. However, other material combinations optimized for specific detection wavelengths and types of radiation are also possible. Making use of quantum confinement to increase the exciton energies of compounds containing elements with high atomic numbers, which is of interest for X-ray detection, appears to be a promising direction for future research.

METHODS

The bare CdSe nanowire devices were prepared by the EC-SLS method according to Dorn *et al.*[14] and were subsequently annealed under vacuum at 350 °C for 30 min in a nitrogen glovebox. Nanocrystals were prepared according to standard wet-chemical techniques (see Supporting Information for details) and added to the nanowire mat by drop-casting from a 10:1 hexane/octane solution. The samples were held under vacuum during confocal photocurrent scanning with a 60× air objective (Nikon) mounted on an *xyz*-piezo stage (PI). An argon-ion laser (Coherent, Spectra) with a switchable wavelength between 650 and 514 nm served as a continuous wave light source. The diameter of the laser focus was approximately 0.4−0.5 μm. We biased the device with a digital voltage source (Yokogawa 7651 Programmable DC Source) and used an IV converter (DL Instruments, LLC) in conjunction with a multimeter (Agilent 34401A) to measure the induced photocurrent.

Acknowledgment. This work was supported by the DOE Center for Excitonics, an Energy Frontiers Research Center funded by the U.S. Department of Energy, Office of Basic Energy Sciences (DE-SC0001088), as well as NSEC (DMR-D213282) and the NSF-MRSEC Program at MIT, and made use of its shared experimental facilities as well as Harvard NSF-NSEC facilities. The authors declare that they have no conflicting financial interests. A.D. conceived and designed the project and wrote the manuscript. A.D. and D.B.S. conducted experiments; D.K.H. and H.H. participated in materials synthesis, and all authors analyzed and discussed the data and commented on the manuscript.

Supporting Information Available: Nanocrystal synthesis, thickness determination of drop-cast nanocrystal films by atomic force microscopy, scanning electron microscope images of nanowires before and after drop-casting nanocrystals, current−voltage characteristic under illumination, and determination of nonradiative exciton transfer rates. This material is available free of charge via the Internet at http://pubs.acs.org.

REFERENCES AND NOTES

1. Leatherdale, C. A.; Kagan, C. R.; Morgan, N. Y.; Empedocles, S. A.; Kastner, M. A.; Bawendi, M. G. Photoconductivity in CdSe Quantum Dot Solids. *Phys. Rev. B* **2000**, *62*, 2669–2680.
2. Ginger, D. S.; Greenham, N. C. Charge Injection and Transport in Films of CdSe Nanocrystals. *J. Appl. Phys.* **2000**, *87*, 1361–1368.
3. Oertel, D. C.; Bawendi, M. G.; Arango, A. C.; Bulovic, V. Photodetectors Based on Treated CdSe Quantum-Dot Films. *Appl. Phys. Lett.* **2005**, *87*, 213505.
4. Konstantatos, G.; Howard, I.; Fischer, A.; Hoogland, S.; Clifford, J.; Klem, E.; Levina, L.; Sargent, E. H. Ultrasensitive Solution-Cast Quantum Dot Photodetectors. *Nature* **2006**, *442*, 180–183.
5. Konstantatos, G.; Sargent, E. H. Nanostructured Materials for Photon Detection. *Nat. Nanotechnol.* **2010**, *5*, 391–400.
6. Yu, D.; Wang, C. J.; Wehrenberg, B. L.; Guyot-Sionnest, P. Variable Range Hopping Conduction in Semiconductor Nanocrystal Solids. *Phys. Rev. Lett.* **2004**, *92*, 216802.
7. Lu, S.; Madhukar, A. Nonradiative Resonant Excitation Transfer from Nanocrystal Quantum Dots to Adjacent Quantum Channels. *Nano Lett.* **2007**, *7*, 3443–3451.
8. Lu, S. Y.; Lingley, Z.; Asano, T.; Harris, D.; Barwicz, T.; Guha, S.; Madhukar, A. Photocurrent Induced by Nonradiative Energy Transfer from Nanocrystal Quantum Dots to Adjacent Silicon Nanowire Conducting Channels: Toward a New Solar Cell Paradigm. *Nano Lett.* **2009**, *9*, 4548–4552.
9. Yu, Y. H.; Kamat, P. V.; Kuno, M. A CdSe Nanowire/Quantum Dot Hybrid Architecture for Improving Solar Cell Performance. *Adv. Funct. Mater.* **2010**, *20*, 1464–1472.
10. Zebli, B.; Vieyra, H. A.; Carmeli, I.; Hartschuh, A.; Kotthaus, J. P.; Holleitner, A. W. Optoelectronic Sensitization of Carbon Nanotubes by CdTe Nanocrystals. *Phys. Rev. B* **2009**, *79*, 205402.
11. Shafran, E.; Mangum, B. D.; Gerton, J. M. Energy Transfer from an Individual Quantum Dot to a Carbon Nanotube. *Nano Lett.* **2010**, *10*, 4049–4054.
12. Walker, B. J.; A., D.; Bulovic, V.; M.G., B. Color-Selective Photocurrent Enhancement in Coupled J-Aggregate/Nanowires Formed in Solution. *Nano Lett.* **2011**, *11*, 2655–2659.
13. van Kouwen, M. P.; van Weert, M. H. M.; Reimer, M. E.; Akopian, N.; Perinetti, U.; Algra, R. E.; Bakkers, E. P. A. M.; Kouwenhoven, L. P.; Zwiller, V. Single Quantum Dot Nanowire Photodetectors. *Appl. Phys. Lett.* **2010**, *97*, 113108.
14. Dorn, A.; Wong, C. R.; Bawendi, M. G. Electrically Controlled Catalytic Nanowire Growth from Solution. *Adv. Mater.* **2009**, *21*, 3479.
15. Dorn, A.; Allen, P. M.; Bawendi, M. G. Electrically Controlling and Monitoring InP Nanowire Growth from Solution. *ACS Nano* **2009**, *3*, 3260–3265.
16. Trentler, T. J.; Hickman, K. M.; Goel, S. C.; Viano, A. M.; Gibbons, P. C.; Buhro, W. E. Solution−Liquid−Solid Growth of Crystalline III−V Semiconductors: An Analogy to Vapor−Liquid−Solid Growth. *Science* **1995**, *270*, 1791–1794.
17. Ouyang, L.; Maher, K. N.; Yu, C. L.; McCarty, J.; Park, H. Catalyst-Assisted Solution−Liquid−Solid Synthesis of CdS/CdSe Nanorod Heterostructures. *J. Am. Chem. Soc.* **2007**, *129*, 133–138.
18. Wang, F. D.; Buhro, W. E. An Easy Shortcut Synthesis of Size-Controlled Bismuth Nanoparticles and Their Use in the SLS Growth of High-Quality Colloidal Cadmium Selenide Quantum Wires. *Small* **2010**, *6*, 573–581.
19. Li, Z.; Kurtulus, O.; Fu, N.; Wang, Z.; Kornowski, A.; Pietsch, U.; Mews, A. Controlled Synthesis of CdSe Nanowires by Solution−Liquid−Solid Method. *Adv. Funct. Mater.* **2009**, *19*, 3650–3661.
20. Yu, H.; Li, J. B.; Loomis, R. A.; Gibbons, P. C.; Wang, L. W.; Buhro, W. E. Cadmium Selenide Quantum Wires and the Transition from 3D to 2D Confinement. *J. Am. Chem. Soc.* **2003**, *125*, 16168–16169.
21. Singh, A.; Li, X.; Protasenko, V.; Galantai, G.; Kuno, M.; Xing, H.; Jena, D. Polarization-Sensitive Nanowire Photodetectors

Based on Solution-Synthesized CdSe Quantum-Wire Solids. *Nano Lett.* **2007**, *7*, 2999–3006.
22. Jiang, Y.; Zhang, W. J.; Jie, J. S.; Meng, X. M.; Fan, X.; Lee, S. T. Photoresponse Properties of CdSe Single-Nanoribbon Photodetectors. *Adv. Funct. Mater.* **2007**, *17*, 1795–1800.
23. Balasubramanian, K.; Burghard, M.; Kern, K.; Scolari, M.; Mews, A. Photocurrent Imaging of Charge Transport Barriers in Carbon Nanotube Devices. *Nano Lett.* **2005**, *5*, 507–510.
24. Ahn, Y.; Dunning, J.; Park, J. Scanning Photocurrent Imaging and Electronic Band Studies in Silicon Nanowire Field Effect Transistors. *Nano Lett.* **2005**, *5*, 1367–1370.
25. Gu, Y.; Kwak, E. S.; Lensch, J. L.; Allen, J. E.; Odom, T. W.; Lauhon, L. J. Near-Field Scanning Photocurrent Microscopy of a Nanowire Photodetector. *Appl. Phys. Lett.* **2005**, *87*, 043111.
26. Freitag, M.; Tsang, J. C.; Bol, A.; Yuan, D. N.; Liu, J.; Avouris, P. Imaging of the Schottky Barriers and Charge Depletion in Carbon Nanotube Transistors. *Nano Lett.* **2007**, *7*, 2037–2042.
27. Hernandez-Martinez, P. L.; Govorov, A. O. Exciton Energy Transfer between Nanoparticles and Nanowires. *Phys. Rev. B* **2008**, *78*, 035314.
28. Milbrath, B. D.; Peurrung, A. J.; Bliss, M.; Weber, W. J. Radiation Detector Materials: An Overview. *J. Mater. Res.* **2008**, *23*, 2561–2581.
29. Dujardin, C.; Amans, D.; Belsky, A.; Chaput, F.; Ledoux, G.; Pillonnet, A. Luminescence and Scintillation Properties at the Nanoscale. *IEEE Trans. Nucl. Sci.* **2010**, *57*, 1348–1354.